On Electronic Structure and Geometry of MoX_2 (X = S, Se, Te) and Black Phosphorus by *ab initio* Simulation with Various van der Waals Corrections

Yi-Chia Tsai, *Student Member*, Yiming Li, *Member, IEEE*

***Abstract*—To get an accurate prediction of the geometry and electronic structure of two-dimensional materials, the use of functionals for the exchange-correlation and the van der Waals corrections are consequential. We present a more rigorous simulation procedure by adopting different exchange-correlation functionals for geometry relaxation and electronic structure calculation. As the results, by using Perdew-Burke-Ernzerhof (PBE) functional, the geometry and the bandgap of the bulk transition metals dichalcogenides can be satisfied in comparison with the experimental measurement. It should, however, incorporate the Heyd-Scuseria-Ernzerhof (HSE06) functional and DFT-D2 van der Waals correction at the same time to reproduce a close geometry and bandgap of bulk black phosphorus (BP). A large cell calculation for BP, such as contact engineering and doping engineering, can thus take the advantage of accuracy while remains time efficiency.**

***Index Terms*— van der Waals, exchange-correlation functionals, density functional theory, two-dimensional material.**

I. Introduction

Ever since the discovery of graphene, two-dimensional (2D) materials are emerging as a promising candidate to the end-of-road-map silicon-based semiconductor industry [1-3]. 2D materials have a gap between each layer, so called van der Waals gap, where the individual layer bonds with others through a weak van der Waals interaction. Among then, transition metals dichalcogenides (TMDs) and black phosphorus (BP) equip with a layer-dependent and favorable bandgap and a monolayer limit making it potential in the optoelectronic devices. Moreover, the naturally ultra-thin body thickness of these materials prevents the mobility degradation from surface scattering which brings the opportunity to the next-generation nanoelectronics [4], [5]. To get a first-hand prediction to the aforementioned properties, the density functional theory (DFT) with a pseudopotential framework has become a reliable and dominant procedure [6]. Based on the calculated geometry and the electronic structure, the DFT can be further extended, which is the density functional perturbation theory (DFPT), to simulate the phonon-interaction [7], the impact of the electric field [8], the dielectric constant [9]. Therefore, it is an consequential task to approach the accurate geometry and the electronic structure of the desire material at the first place. However, the exchange-correlation energy and the non-local van der Waals interaction make the 2D materials hard to be modeled. In the simulation, the conventional local or semi-local DFT is not enough to accurately describe the charge dispersion between van der Waals gap. Although several theoretical researches had been done by adopting the van der Waals corrections [10-13], the impact of van der Waals correction on structural and electrical characteristics remains unclear. Even more important, would it introduce an extra strain on the geometry? Should we need to adopt the geometry relaxed by the van der Waals correction when calculating the electronic structure?

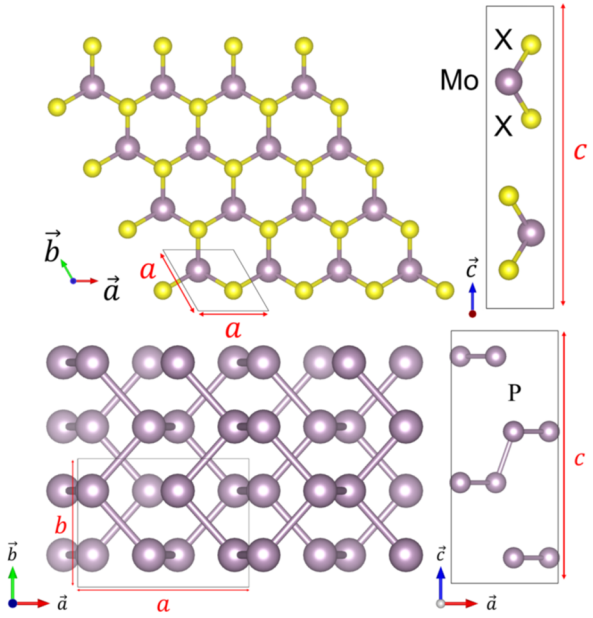

Fig. 1. The top and side view of MoX_2 (above) and BP (below) geometry. *a*, *b*, and *c* are the lattice vectors in three directions.

To solve these questions, we benchmark different types of van der Waals corrections on the 2H phase molybdenum disulfide (MoS_2), molybdenum diselenide ($MoSe_2$), molybdenum telluride ($MoTe_2$), and black phosphorus (BP) by looking at its lattice vectors in the three directions, volume, and bandgap. The bulk structure of these materials is

Yi-Chia Tsai and Yiming Li are with the Parallel and Scientific Computing Laboratory, Department of Electrical and Computer Engineering, Institute of Communications Engineering, National Chiao Tung University, Hsinchu 300, Taiwan (e-mail: ymli@faculty.nctu.edu.tw).

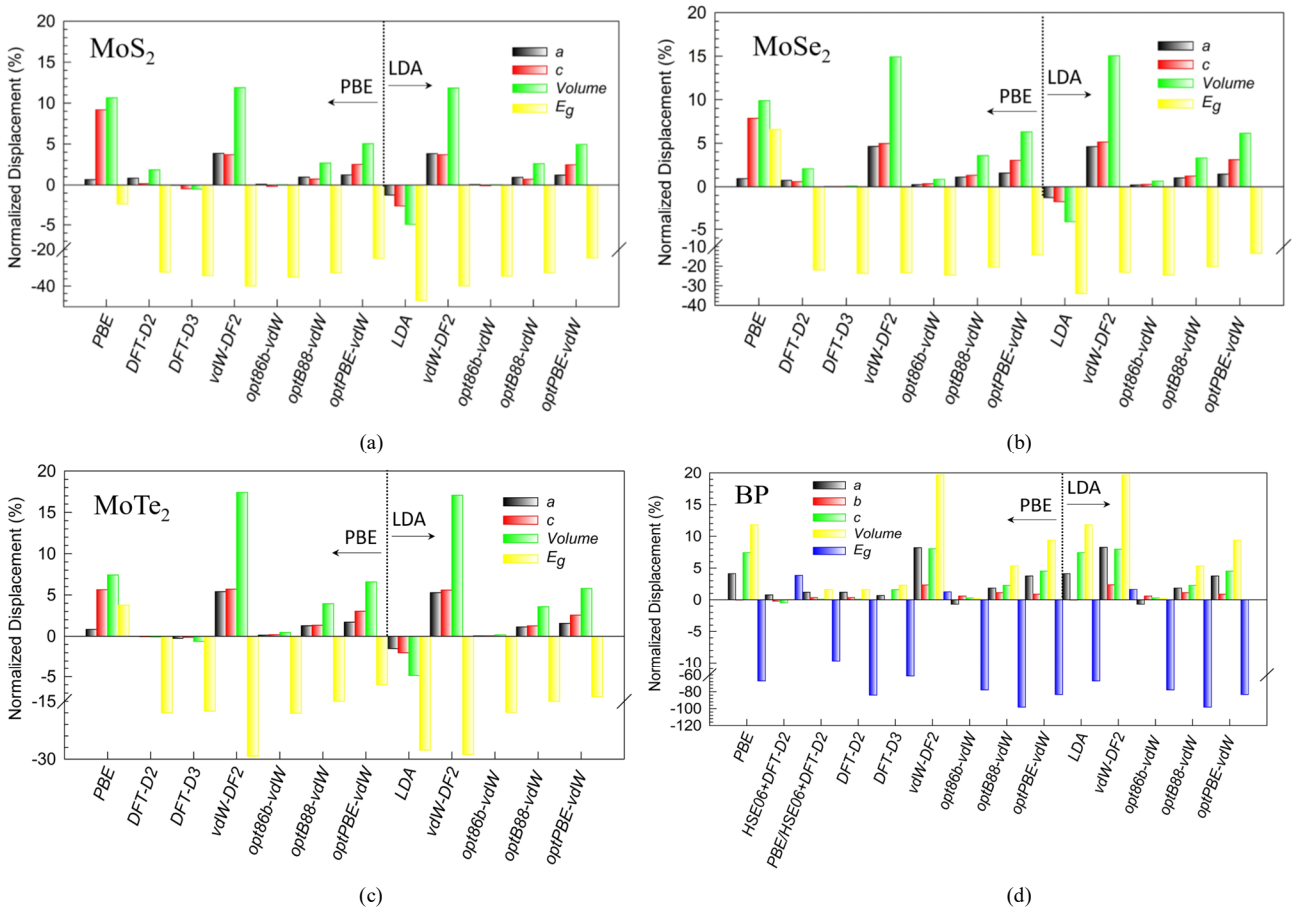

Fig. 2. The normalized displacement in percentage versus different combination of exchange-correlation and van der Waals correction functionals for the bulk (a) MoS_2 (b) $MoSe_2$ (c) $MoTe_2$ (d) BP.

investigated because of the availability and consistency of experimental data.

We find out that the Perdew-Burke-Ernzerhof (PBE) functional without a van der Waals correction can well reproduce the bandgap of the TMDs at the expense of 9% overestimation on the layer-to-layer direction. However, if the one uses the van der Waals correction, the geometry is perfectly reproduced but the bandgap is overestimated by 20%. For the black phosphorus, although DFT-D2 and DFT-D3 van der Waals corrections yield accurate lattice geometries, none of the proposed method bring a close bandgap. By using the hybrid functional and DFT-D2 van der Waals correction, both the geometry and the electrical characteristic match the experiments with a deviation less than 4%.

II. Computational Details

The simulation of TMDs and BP are carried out under the spin-polarized density functional theory framework, where the projector augmented-wave (PAW) pseudopotentials are used for describing the valence electrons. Three commonly used exchange-correlation functionals: Perdew-Burke-Ernzerhof (PBE), local density approximation (LDA), and Heyd-Scuseria-Ernzerhof (HSE06) are applied which are implemented in Vienna *ab initio* Simulation Package (VASP). The van der Waals correction functionals of vdW-DF [14-16] and DFT-D approaches, including opt86b-vdW, optB88-vdW, optPBE-vdW, vdW-DF2, DFT-D2 [17], and DFT-D3 [18], are considered for the different exchange-correlation functionals. The cutoff kinetic-energy of 500 eV is employed for the valence electrons, where the convergence condition for the force acting on each atom and the energy difference are less than 0.01 eVÅ^{-1} and 10^{-6} eV, respectively. The Brillouin zone is sampled with a grid of 12 x 12 x 4 by gamma-centered Monkhorst-Pack algorithm.

To compare the calculated value with the experimental measurement, we use the normalized displacement, which is calculated by x_{cal}/x_{exp}-1, where x_{cal} is the computed lattice vectors, volume, or bandgap (Eg) and x_{exp} is the corresponding experiment reference listed in Table 1. It measured the difference between the simulation and experiment in percentage.

III. Results and Discussion

We use lattice vectors and bandgap to represent the structural and electronic characteristics of TMDs and BP.

Table 1. List of the experimental measurements on the structural property and bandgap.

Materials	*a* (Å)	*b* (Å)	*c* (Å)	*V* (Å^3)	*Eg* (eV)
MoS_2	3.16	3.16	12.295	106.39	1.29
$MoSe_2$	3.29	3.29	12.9	120.79	1.09
$MoTe_2$	3.52	3.52	13.964	149.75	0.9
BP	4.37	3.31	10.473	151.77	0.31

Fig. 1 shows the top and side view of MoX_2 (above) and BP (below) geometry. Due to the symmetry of the primitive cell of MoX_2, two in-plane lattice vectors are equal and denotes as *a*; whereas the lattice vector in the layer-to-layer direction (*z* direction) denotes as *c*. For BP, the lattice vectors of *a*, *b*, and *c* are parallel to the *x* (armchair), *y* (zigzag), and *z* axis, respectively. In the upper figure, the yellow and purple circles are the chalcogen (X=S, Se, Te) and molybdenum (Mo) atoms; while all purples circles in the lower figure are the phosphorus (P) atoms.

Figs. 2 are the normalized displacement of lattice vectors, volume, and bandgap with a different combination of functionals on the bulk MoS_2, $MoSe_2$, $MoTe_2$, and BP, respectively. As shown in the Fig. 2(a), the opt86b-vdW van der Waals correction is able to recreate the experimental geometry regardless of the used exchange-correlation functional. Both PBE and LDA exchange-correlation functionals yield the similar results if the vdW-DF van der Waals correlation functional is adopted because the correlation functional of vdW-DF is attribute to the mixture of the LDA correlation functional and the non-local correlation functional [19], where the exchange functional of generalized gradient approximation (GGA) is exploited. Despite the fact that the lattice vectors and volume match with the experiment, the bandgap is underestimated by about 40% (0.52 eV) because an extra strain is imposed from *z* direction. The similar phenomenon can be observed for all applied van der Waals correction functionals. To get a close bandgap in comparison with the experiment, a pure PBE exchange-correlation functional without any van der Waals correction, which merely underestimates the bandgap of 2% (0.026 eV), is necessary. The significant difference between the geometry and bandgap under the same exchange-correlation functional means that it might risk of losing accuracy on electrical properties if the geometry is fully optimized by a van der Waals correlation functional. However, the significant underestimation of bandgap by van der Waals correction does not work for a monolayer limit because the overestimation of geometry is mainly in the layer-to-layer direction. To be more specific, originally, the bandgap decreases because the lattice vector in the *z* direction is compressed by using opt86b-vdW van der Waals correction. In the monolayer limit, the van der Waals gap does not exist, therefore the strain from the *z* direction is insignificant and the bandgaps obtained by the PBE and opt86b-vdW are the same.

In the Fig. 2(b), different from MoS_2, the optimal van der Waals correction functional for the geometry of $MoSe_2$ is the DFT-D3 van der Waals correction. The DFT-D3 perfectly

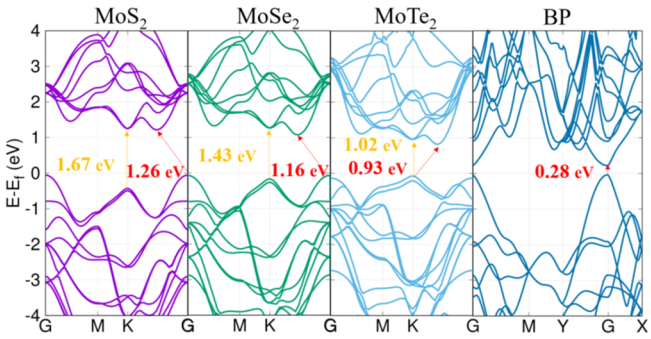

Fig. 3. The calculated electronic structure by using the best combination of functionals. MoS_2, $MoSe_2$, $MoTe_2$ are calculated by unified PBE functional; whereas the band structure of BP is calculated by HSE06+DFT-D2 but using the geometry from PBE+DFT-D2. The indirect (red) and direct (yellow) bandgaps are shown in the figure.

reproduces the experimental result. However, the extra strain is introduced as well and the bandgap is underestimated by 30% (0.3 eV). Same as the MoS_2, a close bandgap is retained by using the pure PBE exchange-correlation functional without any van der Waals correction. The difference between MoS_2 and $MoSe_2$ is that the bandgap is overestimated by 6% (0.06 eV) when the pure PBE is adopted. $MoTe_2$, on the other hand, has an optimal exchange-correlation of DFT-D2 van der Waals correction functional for the geometry relaxation, as shown in Fig. 2(c). The deviation of lattice vectors and volume from the experiment is less than 1% but the bandgap is underestimated by 16% (0.14 eV). By using the intrinsic PBE exchange-correlation functional, the bandgap is merely overestimated by 3% (0.03 eV). Nevertheless, the same old trick cannot play again on BP as shown in the Fig. 2(d). By using the DFT-D2 van der Waals correction, the lattice vectors in three directions are consistent with the experimental measurement, the bandgap is underestimated by 90% (0.28 eV). Even using the intrinsic PBE exchange-correlation functional, the bandgap is still been underestimated by 60% (0.19 eV). Since there is no available strategy to recover the bandgap, we then climb up the Jacob's ladder [20] to seek for the improvement. First, we employed the HSE06 hybrid functional with DFT-D2 van der Waals correction for a more accurate calculation, the lattice vectors in three directions are matched with the experiment, most important of all, the bandgap is 4% (0.01 eV) overestimated only. However, the computational cost is very expensive for a supercell calculation, such as contact engineering and doping engineering, due to the complexity of Hartree–Fock exact exchange functional. To further optimize the computational time, a separated treatment for the geometry relaxation and electronic calculation is proposed. Because the geometry obtained by the integration of PBE and DFT-D2 functional is similar to the one retrieved from the combination of HSE06 and DFT-D2 functional, where the volume of the unit cell is only 1.5% in difference, therefore we can simply use the PBE and DFT-D2 functional for the geometry relaxation. When it comes to the electronic structure calculation, the HSE06 is exploited and started from the pre-converged geometry by the

PBE and DFT-D2 functional. Surprisingly, the bandgap is only been undervalued by 9.6% (0.03 eV). It is worth noting that the bandgap of bulk BP varied from 0.3 to 0.35 eV [21-24], therefore, even though the deviation is large in percentage, the absolute difference of 0.03 eV is quite accurate compared with the deviation between the experiments. Also, by using the mixed functional in the different stage, researcher can easily save the computational time without sacrificing too much accuracy. The calculated electronic structures of MoS_2, $MoSe_2$, $MoTe_2$, and BP are demonstrated in Fig. 3. The use of functionals are applied as proposed, the direct (yellow) and indirect (red) bandgap are in agreement with experiments [25-27].

IV. Conclusion

In the geometry optimization, there is no universal approach, instead, opt86b-vdW, DFT-D3, DFT-D2, and the integration of HSE06 and DFT-D2 show a best fit to MoS_2, $MoSe_2$, $MoTe_2$, and BP, respectively. Luckily, for TMDs, the PBE functional can retrieve the correct bandgap (smaller than 5%) without sacrificing too much accuracy on geometry (smaller than 10%). For the electronic calculation of BP, although the van der Waals correction gives a satisfactory geometry, the bandgap is underestimated for more than 60%. It can be improved by using the integration of HSE06 and DFT-D2 starting with the relaxed structure by the mixture of PBE and DFT-D2 van der Waals correction. The bandgap difference between this approach and experiment is smaller than 0.03 eV and the difference of unit cell's volume is only 2%.

Acknowledgment

This work was supported in part by the MOST, Taiwan, under grant 105-2221-E-009-132 and a TSMC grant in 2016-2017.

References

[1] M. Akhtar, G. Anderson, R. Zhao, A. Alruqi, J. E. Mroczkowska, G. Sumanasekera, and J. B. Jasinski, "Recent advances in synthesis, properties, and applications of phosphorene," *npj 2D Mat. and Appl*, vol. 1, no. 5, pp. 1–13, 2017.

[2] L. Li, Y. Yu, G. J. Ye, Q. Ge, X. Ou, H. Wu, D. Feng, X. H. Chen, and Y. Zhang, "Black phosphorus field-effect transistors," Nat. Nano., vol. 9, no. 5, pp. 372–377, 2014.

[3] G. R. Bhimanapati *et al.*, "Recent advances in two-dimensional materials beyond graphene," *ACS Nano*, vol. 9, no. 12, pp. 11509–11539, 2015.

[4] L. Li, M. Engel, D. B. Farmer, S.-j. Han, and H.-S. P. Wong, "High-performance p-type black phosphorus transistor with scandium contact," *ACS Nano*, vol. 10, no. 4, pp. 4672–4677, 2016.

[5] X. Ling, H. Wang, S. Huang, F. Xia, and M. S. Dresselhaus, "The renaissance of black phosphorus," *Proc. Natl. Acad. Sci.*, vol. 112, no. 15, pp. 4523–4530, 2015.

[6] A. Jain, Y. Shin, and K. A. Persson, "Computational predictions of energy materials using density functional theory," *Nat. Rev. Mat.*, vol. 1, p. 15004, 2016.

[7] O. D. Restrepo, K. Varga, and S. T. Pantelides, "First-principles calculations of electron mobilities in silicon: Phonon and Coulomb scattering," *Appl. Phys. Lett.*, vol. 94, p. 212103, 2009.

[8] A. Kuc and T. Heine, "The electronic structure calculations of two-dimensional transition-metal dichalcogenides in the presence of external electric and magnetic fields," *Chem. Soc. Rev.*, vol. 44, pp. 2603–2614, 2015.

[9] S. Guan, S. A. Yang, L. Zhu, J. Hu, and Y. Yao, "Electronic, dielectric, and plasmonic properties of two-dimensional electride materials X_2N (X=Ca, Sr): A first-principles study," *Sci. Rep.*, vol. 5, p. 12285, 2015.

[10] J. Kang, W. Liu, D. Sarkar, D. Jena, and K. Banerjee, "Computational study of metal contacts to monolayer transition-metal dichalcogenide semiconductors," *Phys. Rev. X*, vol. 4, no. 3, p. 031005, 2014.

[11] K. Gong, L. Zhang, W. Ji, and H. Guo, "Electrical contacts to monolayer black phosphorus: A first-principles investigation," *Phys. Rev. B*, vol. 90, no. 12, p. 125441, 2014.

[12] Y. Cai, G. Zhang, and Y.-W. Zhang, "Layer-dependent band alignment and work function of few-layer phosphorene," *Sci. Rep.*, vol. 4, p. 6677, 2014.

[13] Y. Pan *et al.*, "Monolayer phosphorene–metal contacts," *Chem. Mat.*, vol. 28, no. 7, pp. 2100–2109, 2016.

[14] M. Dion, H. Rydberg, E. Schröder, D. C. Langreth, and B. I. Lundqvist, "Van der Waals density functional for general geometries," *Phys. Rev. Lett.*, vol. 92, no. 24, p. 246401, 2004.

[15] J. Klimeš, D. R. Bowler, and A. Michaelides, "Van der Waals density functionals applied to solids," *Phys. Rev. B*, vol. 83, no. 19, p. 195131, 2011.

[16] T. Thonhauser, V. R. Cooper, L. Shen, A. Puzder, P. Hyldgaard, and D. C. Langreth, "Van der Waals density functional: Self-consistent potential and the nature of the van der Waals bond," *Phys. Rev. B*, vol. 76, no. 12, p. 125112, 2007.

[17] S. Grimme., "Semiempirical gga-type density functional constructed with a long-range dispersion correction," *J. Comp. Chem.*, vol. 27, no. 15, pp. 1787–1799, 2006.

[18] S. Grimme, J. Antony, S. Ehrlich, and S. Krieg, "A consistent and accurate *ab initio* parametrization of density functional dispersion correction (dft-d) for the 94 elements H-Pu," *J. Chem. Phys.*, vol. 132, no. 15, p. 154104, 2010.

[19] J. Klimeš, D. R. Bowler, and A. Michaelides, "Chemical accuracy for the van der Waals density functional," *J. Phys. Condens. Matt.*, vol. 22, no. 2, p. 022201, 2010.

[20] J. P. Perdew, A. Ruzsinszky, and J. Tao, "Prescription for the design and selection of density functional approximations: More constraint satisfaction with fewer fits," J. Chem. Phys., vol. 123, no. 6, p. 062201, 2005.

[21] R. W. Keyes, "The electrical properties of black phosphorus," *Phys. Rev.*, vol. 92, p. 580, 1953.

[22] D. Warschauer, "Electrical and optical properties of crystalline black phosphorus," *J. Appl. Phys.*, vol. 34, p. 1853, 1963.

[23] Y. Maruyama and S. Suzuki, "Synthesis and some properties of black phosphorus single crystals," *Physica B + C*, vol. 105, p. 99, 1981.

[24] Y. Akahama, S. Endo, and S.-i. Narita, "Electrical properties of black phosphorus single crystals," *J. Phys. Soc. Jpn.*, vol. 52, p. 2148, 1983.

[25] K. Kam, B. Parkinson, "Detailed photocurrent spectroscopy of the semiconducting group VIB transition metal dichalcogenides," *J. Phys. Chem.*, vol. 86, p. 463, 1982.

[26] T. Böker, R. Severin, A. Müller, C. Janowitz, R. Manzke, D. Voß, P. Krüger, A. Mazur, and J. Pollmann, "Band structure of MoS_2, $MoSe_2$, and α-$MoTe_2$: Angle-resolved photoelectron spectroscopy and ab initio calculations," *Phys. Rev. B*, vol. 64, p. 235305, 2001.

[27] Wyckoff R W G, Crystal Structures 1, 280 (1963).